Fatty acid binding protein 5 mediates the uptake of fatty acids, but not drugs, into human brain endothelial cells

Gordon S. Lee[1], Yijun Pan[1], Martin J. Scanlon [2], Christopher J. H. Porter[1,3], ***Joseph A. Nicolazzo[1]****

[1]Drug Delivery, Disposition and Dynamics, Monash Institute of Pharmaceutical Sciences, Monash University, Parkville, Victoria, Australia

[2]Medicinal Chemistry, Monash Institute of Pharmaceutical Sciences, Monash University, Parkville, Victoria, Australia

[3]ARC Centre of Excellence in Convergent Bio-Nano Science and Technology, Monash Institute of Pharmaceutical Sciences, Monash University, Parkville, Victoria, Australia

Corresponding author email: joseph.nicolazzo@monash.edu

Running title: FABP5 in brain endothelial cell uptake

* **Corresponding author:** Dr. J. A. Nicolazzo, Drug Delivery, Disposition and Dynamics, Monash Institute of Pharmaceutical Sciences, Monash University, 381 Royal Parade, Parkville, Victoria 3052, Australia

Telephone No.: +61 3 9903 9605

Fax No.: +61 3 9903 9583

Abstract

The purpose of this study was to examine the involvement of fatty acid binding protein 5 (FABP5), a lipid binding protein expressed at the blood-brain barrier (BBB), in fatty acid and drug uptake into human brain endothelial cells. Following transfection with siRNA against hFABP5, human brain endothelial cell (hCMEC/D3) uptake of lipophilic ligands with varying affinity to FABP5 was assessed with intracellular concentrations quantified by liquid scintillation counting, HPLC or LCMS/MS. The *in situ* BBB transport of [^{3}H]-diazepam was also assessed in wild type (WT) and FABP5-deficient mice. hFABP5 siRNA reduced FABP5 expression in hCMEC/D3 cells by 39.9 ± 3.8% (mRNA) and 38.8 ± 6.6% (protein) (mean ± SEM), leading to a reduction in uptake of [^{14}C]-lauric acid, [^{3}H]-oleic acid and [^{14}C]-stearic acid by 37.5 ± 8.8%, 41.7 ± 11.6% and 50.7 ± 13.6%, respectively, over 1 min. No significant changes in [^{14}C]-diazepam, pioglitazone and troglitazone uptake were detected following FABP5 knockdown in hCMEC/D3 cells. Similarly, no difference in BBB transport of [^{3}H]-diazepam was observed between WT and FABP5-deficient mice. Therefore, while FABP5 facilitates brain endothelial cell uptake of fatty acids, it has limited effects on brain endothelial cell uptake and BBB transport of drugs with lower affinity for FABP5.

Keywords

Blood-brain barrier; fatty acid uptake; drug uptake; fatty acid binding protein 5

Abbreviations

ANS – 8-Anilinonaphthalene-1-sulfonic acid, BBB – blood-brain barrier, BCEC – brain capillary endothelial cells, CNS – central nervous system, DHA – docosahexaenoic acid, FABP – fatty acid binding protein, hCMEC/D3 – immortalized human brain endothelial cells, iLBP – intracellular lipid binding proteins

Introduction

The transport of drugs from the bloodstream into the brain is a necessary step in the pharmacological treatment of neurological and neurodegenerative diseases (1-3). However, the transfer of endogenous ligands and drugs from within the cerebral microvasculature into the central nervous system (CNS) is often restricted due to the presence of the blood-brain barrier (BBB), a single layer of highly specialized endothelial cells which line brain capillaries (4). The restrictive nature of the barrier results from two major factors: 1) Inter-endothelial tight junctions between brain capillary endothelial cells (BCECs) preventing the paracellular diffusion of highly water soluble molecules into the brain parenchyma (5) and 2) efflux transporter proteins, such as P-glycoprotein (P-gp) and breast cancer resistance protein (BCRP) and metabolic enzymes within BCECs restricting the transcellular transport of both endogenous and exogenous molecules (6). Drugs and endogenous molecules that permeate the BBB effectively, typically have physicochemical properties consistent with good passive permeability across BCECs (i.e. low molecular weight and moderate lipophilicity) (7), and/or contain structural features that allow them to undergo carrier-mediated transport into BCECs (7, 8).

A fundamental step in the translocation of lipophilic drugs across the BBB, regardless of whether they permeate the luminal membrane of BCECs via passive diffusion or by a carrier-mediated transport protein, is their subsequent passage through the aqueous cytoplasm of BCECs (7, 9). Once associated with the lipophilic luminal membrane of BCECs, the desorption of lipophilic drugs from this membrane into and across the aqueous cytoplasm to the abluminal membrane is likely to be thermodynamically unfavourable and may pose as a significant rate limiting step in the transport of these poorly-water soluble

drugs across the BBB (10, 11). The same situation is likely faced by endogenous lipophilic molecules permeating the BBB, including fatty acids. Fatty acids have been shown to permeate the lipophilic luminal membrane of brain endothelial cells by both passive diffusion and active transport mechanisms. In particular, fatty acid transport protein 1 has been implicated in the uptake of fatty acids such as docosahexaenoic acid (DHA) (12) and for esterified DHA, a significant involvement of a relatively new transporter, Mfsd2a has been implicated (13). Regardless of the processes governing the luminal membrane transport of fatty acids, the subsequent movement of molecules from the luminal membrane to the abluminal membrane has been largely ignored. In many cell types, the transfer of endogenous lipophilic entities, such as fatty acids, from plasma membranes into the cytosol, their cytosolic solubilisation and their subsequent diffusion have been demonstrated to be facilitated by the aid of intracellular lipid binding proteins (iLBPs) (14, 15). Fatty acid binding proteins (FABPs) represent one class of cytosolic proteins belonging to the iLBP family (16, 17). The human FABP family consists of 9 isoforms originally named based on the tissue in which they were first identified. This traditional nomenclature is however somewhat misleading as many tissues and cell types have been found to express multiple FABP isoforms. A numerical system is now used instead to refer to the 9 isoforms (16, 17). As suggested by their name, FABPs bind to fatty acids and thereby act as cellular chaperones for fatty acids in the cytoplasm (17). FABPs are found most highly expressed in tissues with high demand for fatty acid consumption (18-20). While FABP3, FABP5 and FABP7 have been found to be expressed in neurons and other brain parenchymal cells (21), it is only recently, that the expression and function of FABPs at the BBB have been investigated.

FABP5 has been found to be expressed in primary human BCECs (22) and more recently, we have shown expression of FABP3, FABP4 and FABP5 in an immortalized human brain endothelial cell line (hCMEC/D3 cells) (23) and confirmed FABP5 expression at the mouse BBB (24). Given the high expression of FABP5 at the human and murine BBB, we and others have assessed the functional role of FABP5 in trafficking various fatty acids across the aqueous cytoplasm of human BCECs (24-26). Genetic downregulation of FABP5 in primary human BCECs resulted in a ~75%, ~ 46% and ~50% reduction in the transport of palmitic, oleic and linoleic acid, respectively (25). Similarly, genetic knockdown of FABP5 in hCMEC/D3 cells has been demonstrated to result in a 14.1% reduction in DHA uptake (24). The importance of FABP5 in BCEC uptake and BBB transport of DHA has been further investigated using mice lacking FABP5. In these studies the uptake of [^{14}C]-DHA was reduced by 48.4% in BCECs from FABP5-deficient (-/-) mice relative to BCECs from wild type (WT) mice (26), and furthermore, the *in situ* BBB transport of [^{14}C]-DHA was reduced 36.7% relative in FABP5-/- mice relative to WT mice. This reduction in BBB transport of [^{14}C]-DHA was associated with an attenuation in endogenous brain levels of DHA and, realising the important role that DHA plays in the maintenance of cognitive function, cognitive dysfunction was observed in FABP5-/- mice (26). It is therefore clear that FABP5 plays a significant role in the cytoplasmic trafficking of various endogenous fatty acids, however, whether this phenomenon extends to the trafficking of lipophilic drugs that bind FABP5 remains to be investigated. It has been shown that FABPs expressed at the small intestine have the capacity to traffic drugs across this membrane (15, 27, 28), and therefore, FABPs at the BBB may play a similar role.

We have previously demonstrated that the three FABP isoforms present at the human BBB (FABP3, FABP4 and FABP5) are able to bind to various drugs, including benzodiazepines, fibrates, fenamates, thiazolidinediones and propionic acid derived non-steroidal inflammatory drugs in an isoform specific manner and with varying affinities (23). Given that FABP5 has been shown to be important in the cytoplasmic trafficking of fatty acids that bind FABP5 with high affinity, and that FABP5 binds to a wide panel of lipophilic drugs (23), the aim of the present study was to investigate whether FABP5 exhibits a functional role in facilitating the uptake of drugs with varying binding affinity to FABP5. Using hCMEC/D3 cells, a genetic knockdown approach was taken to investigate the involvement of FABP5 in the uptake of 3 drugs with varying affinity to FABP5 (diazepam, pioglitazone and troglitazone) **(Table I)**. As positive controls and to ensure that genetic knockdown in FABP5 resulted in functional deficiency in FABP5, the hCMEC/D3 uptake of 3 fatty acids (lauric, oleic, and stearic acid) was assessed. For one drug (diazepam), *in vitro* studies were complemented with *in situ* studies, with the BBB transport of diazepam assessed in WT and FABP5-/- mice.

Materials and methods

Materials

Cultureware was purchased from Corning Life Sciences (Tewksbury, MA). EBM-2 media and EGM-2 Single Quots Kit were purchased from Lonza (Walkersville, MD) and rat tail collagen type I was purchased from BD Biosciences (Bedford, MA). Penicillin-streptomycin and foetal bovine serum were obtained from Invitrogen (Penrose, Auckland, New Zealand). Dulbecco's Phosphate–buffered saline (D-PBS) and Pierce BCA protein assay kit were purchased from Life Technologies (Mulgrave, Victoria, Australia). Bradford reagent and Precision Plus Protein Kaleidoscope® ladder were purchased from BioRad (Hercules, CA). HiPerfect transfection reagent, hFABP5 FlexiTube siRNA (SI03145835) and Taqman primers and probes for hFABP3 (Hs00269758_m1), hFABP4 (Hs01086177_m1), hFABP5 (Hs02339439_g1) and glyceraldehyde 3-phosphate dehydrogenase (GAPDH) (Hs02758991_g1) were purchased from Applied Biosystems (Foster City, CA). Rabbit anti-FABP5 polyclonal antibody and mouse anti-β-actin polyclonal antibody were obtained from Abcam (Cambridge, MA) and the secondary goat anti-mouse (800 nm) and donkey anti-rabbit (680 nm) antibodies were obtained from Licor (Lincoln, NE). [^{3}H]-diazepam, [^{14}C]-diazepam, [^{14}C]-lauric acid, [^{3}H]-oleic acid, [^{14}C]-sucrose and [^{14}C]-stearic acid were purchased from American Radiolabelled Chemical Inc. (St. Louis, MO). Ultima Gold liquid scintillation cocktail and scintillation vials were purchased from Perkin Elmer Life Sciences (Boston, MA). Pioglitazone and troglitazone were purchased from Adipogen (San Diego, CA). Thiazolyl blue tetrazolium bromide (MTT reagent) and Supelco Ascentis® Express C_{18} column were purchased from Sigma Aldrich (St Louis, MO), whereas the Phenomenex Luna C18(2) column was purchased

from Phenomenex (Torrance, CA). Dimethyl sulfoxide (DMSO) was purchased from EMD chemicals (San Diego, CA). Acetonitrile and methanol were of analytical grade and were purchased from Merck KGaA (Darmstadt, Germany). Milli-Q water was obtained from a Milli-Q water purification system (Millipore, Milford, MA) and all other salts and reagents were of the highest purity commercially available.

Culturing of hCMEC/D3 cells

As previously described, hCMEC/D3 cells (passage 30-36) were grown on cultureware coated with rat-tail collagen type I in the presence of EBM-2 medium supplemented with growth factors from the EGM-2 Single Quots Kit, penicillin-streptomycin and 2.5% v/v foetal bovine serum; herein simply referred to as the culture media (23, 24). hCMEC/D3 cells were seeded at 50,000 cells/cm^2 in 6, 24 and 96 well plates or at 27,000 cells/cm^2 in T75 flasks. The cells were cultured at 37°C at 5% CO_2/95% O_2 and saturated humidity and the media was replaced every second day. At 80% confluency, cells were split into either 6 well plates for Western blotting and real time reverse transcription polymerase chain reaction (RT-qPCR) experiments, 24 well plates for uptake studies or 96 well plates for MTT experiments.

siRNA transfection of FABP5 in hCMEC/D3 cells

4 hr post seeding, hCMEC/D3 cells were washed twice with prewarmed D-PBS and incubated with serum free culture media for 15 min at 37°C in 5% CO_2/95% O_2 and saturated humidity. In the meantime, FABP5 siRNA complexes were prepared by mixing FABP5 siRNA, target sequence: 5'-AGGAGTTAATTAAGAGAATGA-3', with HiPerfect transfection reagent in a 1:2 ratio (v/v) in serum free culture media. The

complexes were left at room temperature for 10 min. The serum free culture media was then removed from the wells and FABP5 siRNA complexes or transfection reagent alone were added dropwise directly onto the cells. Normal cell culture media was added to dilute the concentration of hFABP5 siRNA complex to the desired concentration of 5 nM. Cells were incubated with the siRNA complexes or transfection reagent for 24 hr at 37°C in 5% CO_2/95% O_2 and saturated humidity. 24 hr post transfection the cells were used for either the MTT assay, RT-qPCR, Western blotting, or uptake studies.

MTT assay

To assess the viability of the hCMEC/D3 cells post transfection, and to ensure that treatments did not lead to overt toxicity, a MTT assay was performed on hFABP5 siRNA transfected cells cultured in 96 well plates, with transfection reagent only-treated cells serving as controls. 24 hr after transfection, plates were washed twice with prewarmed D-PBS and treated with 150 µl of serum free culture media containing 6.25% (v/v) of an 8 mg/ml MTT reagent solution prepared in D-PBS. Plates were wrapped in aluminium foil and left to incubate at 37°C in 5% CO_2/95% O_2 and saturated humidity for 4 hr. The media was then discarded and cells were incubated with 150 µl of DMSO for 30 min. Plates were briefly shaken and the absorbance of each well was measured at 540 nm on a PerkinElmer Enspire plate reader (Boston, MA). Measurements were corrected for background absorbance and the viability of the cells that underwent transfection was determined by calculating the percentage change in absorbance compared to transfection reagent only-treated cells. Furthermore, cells which had been treated with 10% DMSO served as a positive control to confirm that the MTT assay was indeed able to discriminate between live and dead cells.

RT-qPCR for mRNA expression of FABPs in hCMEC/D3 cells

24 hr post transfection, the total RNA from hCMEC/D3 cells was isolated using the Qiagen® RNeasy Mini kit (Hilden, Germany) as per the manufacturer's protocol. As previously described, the concentration and the purity of isolated RNA samples was quantified on a Thermo Scientific® Nanodrop 1000 spectrophotometer (Waltham, MA) (23). RT-qPCR reactions were prepared using the Bio-Rad IScript One-Step® RT-qPCR Kit for Probes (Hercules, CA) as per the manufacturer's protocol. In brief, each reaction mixture contained 100 ng of isolated RNA, Taqman primer and probes at a final concentration of 500 nM and 139 nM, respectively, 12.5 µl of RT-qPCR Master mix and nuclease free water to a final volume of 25 µl. RNAse/DNAse free water was used as a negative control and GAPDH was used as a housekeeping gene. The thermocycling protocol for reverse transcription and DNA amplification was as follows: 10 min at 50°C, 5 min at 95°C followed by 45 cycles of 10 sec at 95°C and 30 sec at 60°C, using a Bio-Rad® CFX96 thermocycler (Hercules, CA). The $2^{-\Delta\Delta CT}$ method was used to quantify the change in hFABP5 mRNA expression between siRNA treated and transfection reagent only treated cells (29). To ensure the siRNA against hFABP5 was specific to this gene and had no impact on the expression of the other two FABPs expressed in hCMEC/D3 cells (23), mRNA expression of FABP3 and FABP4 in siRNA and transfection reagent only treated cells was also measured using the relevant primers and probes.

Protein expression of hFABP5 in hCMEC/D3 cells

24 hr post treatment, hCMEC/D3 cells were washed with D-PBS and lysed at 4°C for 30 min using radio-immunoprecipitation assay (RIPA) buffer (150 mM NaCl, 50 mM

Tris base, 1% v/v Triton X-100, 0.5% w/v sodium deoxycholate, and 0.1% w/v sodium dodecyl sulfate (SDS) supplemented with Roche Complete® Protease inhibitor cocktail tablets (Castle Hill, New South Wales, Australia), pH 8.0). The lysates were collected and centrifuged at 13614 x *g* for 30 min at 4°C. The resulting supernatants were transferred to fresh microcentrifuge tubes. The concentration of protein in the supernatants was quantified using the BCA protein assay kit by comparison to standard solutions of bovine serum albumin (BSA) prepared in RIPA buffer. Protein samples were stored at -20°C until required. In accordance with our previously published protocol for hFABP5 detection in hCMEC/D3 cells, SDS-PAGE was carried out on 15 µg protein samples with a Precision Plus Protein Kaleidoscope® ladder serving as a molecular weight marker (23).The Bio-Rad® Trans-Blot SD electrophoretic transfer cell (Hercules, CA) was employed for semi dry transfer of the separated protein bands onto 0.2 µm nitrocellulose membranes. Membranes were rinsed 3 times with Tris buffered saline (0.05 M Tris HCl, 150 mM NaCl, pH 7.6) containing 0.1% v/v Tween 20 (TBST) and blocked with Licor® blocking buffer (Lincoln, NE) for 2 hr to prevent non-specific binding, after which they were exposed to primary antibodies against hFABP5 (1:100 v/v) and β-actin (1:1000 v/v) for 24 hr. Following rinses with TBST (3 x 10 min), IR active secondary antibodies at 1:30,000 dilution in Licor® blocking buffer were applied for 2 hr, after which membranes were rinsed with TBST (3 x 10 min) and visualized using the Licor® Odyssey scanner (Lincoln, NE). Densitometric analysis was performed using Image J (National Institutes of Health, Bethesda, MD) and the density of the FABP5 band was normalized to the β-actin band in each lane to account for variabilities in loading amounts. The normalized FABP5

expression was compared between siRNA and transfection reagent only treated samples to determine the extent of FABP5 protein downregulation.

Cellular uptake of lipophilic ligands in hCMEC/D3 cells

24 hr post siRNA transfection, siRNA and transfection reagent only treated hCMEC/D3 cells were washed twice with prewarmed D-PBS and then incubated with serum free media in a shaking THERMOstar plate reader (BMG Labtech, Ortenberg, Germany) maintained at 37°C shaking at 200 rpm for 10 min. The serum free media was then removed from the wells and cells were incubated with uptake solution (containing lipophilic ligand). Uptake solutions were prepared by spiking serum free culture media with one of the test compounds, including [^{14}C]-diazepam, [^{14}C]-stearic or [^{14}C]-lauric acid (1 µCi/ml) or [^{3}H]-oleic acid (10 µCi/ml). The specific activity was 70 µCi/µmol for [^{14}C]-diazepam, 60 µCi/µmol for [^{3}H]-oleic acid and 55 µCi/µmol for [^{14}C]-stearic and [^{14}C]-lauric acid. The concentration of the pioglitazone and troglitazone uptake solutions were 40,000 ng/ml and 25,000 ng/ml, respectively. After 5 sec of adding the uptake solution into wells, a 50 µl aliquot of the uptake solution was collected to measure the initial concentration of the lipophilic ligand. At various time points, uptake experiments were ceased by removing all of the uptake solution and the wells were rinsed three times with ice cold D-PBS.

For studies with radioactive ligands, washed cells were incubated with 250 µl of 1M sodium hydroxide per well for 3 hr at 37°C to lyse the cells. 150 µl of the resulting lysate was transferred into a 4 ml scintillation pony vial and was mixed with 75 µl of 2M hydrochloric acid and 2 ml of Ultima Gold scintillation fluid. Vials were vortexed for 30

sec and the radioactivity of the samples was determined in a PerkinElmer 2800TR liquid scintillation counter (Boston, MA). The remaining cell lysate was collected and used to determine the protein concentration of the lysate from each well using the Bradford assay by comparison to BSA standard solutions prepared in 1M NaOH. The concentration of radiolabelled fatty acid in the cell lysate (pmol/ml) was normalized to the protein concentration (mg/ml) and initial concentration of fatty acid within the wells (pmol/ml), resulting in a cell-to-medium ratio (ml/mg).

For studies with non-radiolabelled probes (i.e. pioglitazone and troglitazone), cells were lysed with 200 µl of ice cold RIPA buffer at 4°C for 30 min. To mirror the composition of the calibration standards samples (described below), 50 µl of DMSO was added to the lysates. Lysates were transferred into microcentrifuge tubes and spun at 14000 x *g* at 4°C for 10 min. 50 µl of the supernatant was transferred into a new microcentrifuge tube and mixed with 50 µl of mass spectrum grade acetonitrile (to precipitate proteins) and further centrifuged at 14000 x *g* at 4°C for 10 min. The supernatant was collected and pioglitazone samples were placed in HPLC vials and troglitazone samples were placed in LCMS vials for analysis. The BCA assay was used to quantify the protein concentration of the remaining lysates of each sample, with BSA standard solutions prepared in hCMEC/D3 cell lysate that underwent the same treatment as samples. The cellular uptake of pioglitazone and troglitazone in each well (µg) was normalized against the total protein (µg) content of each well (i.e. as a measure of total cellular content) to account for well to well variation in cell number.

HPLC and LCMS/MS analysis

Preparation of calibration standards:

A stock solution of 500,000 ng/ml of pioglitazone or troglitazone was prepared in DMSO, from which working solutions were prepared (200-40,000 ng/ml for pioglitazone and 10-1000 ng/ml for troglitazone) in serum free media. Calibration standards were prepared by adding 50 µl of each standard solution into wells of siRNA-treated and untreated prewashed hCMEC/D3 cells. Wells were incubated for 30 min and then lysed with 200 µl of ice-cold RIPA buffer at 4°C for 30 min. Lysates were transferred into microcentrifuge tubes and treated exactly as detailed above, then analysed by HPLC or LCMS, as described below. To determine the precision and accuracy of the assays, 6 replicates of individually-prepared calibration standards (prepared at 200, 5000 and 40,000 ng/ml for pioglitazone, and at 100, 1000 and 10000 ng/for troglitazone) were quantified using the relevant assay.

Pioglitazone HPLC conditions

HPLC analysis was carried out on a Shimadzu Prominence HPLC system (Kyoto, Japan). A UV/Vis detector (SPD-20A UV-VIS) was used for the detection of pioglitazone at 254 nm. The separation was undertaken at a controlled temperature of 40°C at a flow rate of 1.2 ml/min, using a Phenomenex Luna C18(2) column (250 mm x 4.60 mm i.d, 5 µm particle size) which was used in series with a guard column of the same packing material. A 50 µl sample was injected onto the column for analysis. The following gradient profile was used for the isolation of a pioglitazone with solvent A containing 10 mM phosphate, pH 2.6, and solvent B containing 100% methanol: 0.00 - 5.00 min, 50% B; 5.00 - 5.10 min, 20% B;

5.10 - 6.50 min; 50% B, 6.50 - 10.00 min, 50% B, 10.00 – 11.00 min, 100% B; 11.00-14.00 min, 100% B; 14.00 – 15.00 min, 50% B, followed by a 5 min equilibration under the initial conditions. The total run time was 20 min and pioglitazone eluted between 6.1 - 7.0 min. The calibration curve relating chromatographic peak area to cellular pioglitazone concentration in treated and untreated hCMEC/D3 cells exhibited good linearity (r^2 of >0.999) over the 200 to 40,000 ng/ml range. The % coefficients of variation (precision) for quality control samples (n= 6) prepared at 200 ng/ml, 5000 ng/ml and 40,000 ng/ml was less than 5.7% in transfection reagent only treated cells and less than 2.7% in siRNA treated cells. The accuracy of the replicates ranged from 99.8 - 104.1% of the nominal concentrations in transfection reagent only treated cells and from 95.7 – 117.0% in siRNA treated cells.

Troglitazone LC/MS/MS conditions

Analysis was carried out on a Shimadzu Nexera UHPLC system coupled to a Shimadzu 8030 tandem quadrupole mass spectrometer containing an electrospray ionization source. To determine the suitable mass spectrometry parameters for detecting troglitazone, a 10 µg/ml solution of troglitazone (prepared in 50% v/v methanol in water from the DMSO stock) was directly applied onto the mass spectrometer. Scan data between m/z 50 - 470 in positive and negative ionization mode were acquired to determine a suitable ionization mode and mass of the troglitazone for fragmentation. A parent mass of 440.05 was selected in the negative ionization mode. A product ion scan of fragments of the deprotonated $[M–H]^-$ ion of troglitazone displayed a clear fragment ion at m/z 177.90. The resolution of troglitazone from cleaned cell samples was performed on a Supelco Ascentis® Express C_{18} column (5 cm x 2.1 mm, 2.7 µm) by gradient elution using solvent A: water,

and solvent B: methanol, at a flow rate of 0.5 ml/min. The injection volume for sample analysis was 20 µl. With a gradient elution method of 0.00 - 0.10 min; 50% B, 0.10 – 3.00 min; 90% B, 3.00 – 4.00 min; 90% B, 4.00 – 5.00 min; 50% B, followed by 2 min equilibration at the initial conditions, troglitazone eluted at 2.7 min. The calibration curve relating chromatographic peak area to cellular troglitazone concentration in treated and untreated hCMEC/D3 cells exhibited good linearity (r^2 of >0.997) over the 100 to 10,000 ng/ml range. The % coefficients of variation for quality control samples (n= 6) prepared at 100 ng/ml, 1000 ng/ml and 10,000 ng/ml were less than 5.1% in transfection reagent only treated cells and less than 4.2% in siRNA treated cells. The accuracy values of these replicates ranged from 80.3 - 100% of the nominal concentrations in transfection reagent only treated cells and from 84.2 – 107.1% in siRNA treated cells, respectively.

BBB transport of [^{3}H]-diazepam in WT and FABP5-/- mice

FABP5-/- mice were generated according to a previously published method and maintained on C57BL/6 background (30). All mice were genotyped for the presence or absence of the FABP5 gene by Transnetyx (Cordova, TN). All animal experiments were approved by the Monash Institute of Pharmaceutical Sciences Animal Ethics Committee and performed in accordance with the National Health and Medical Research Council guidelines for the care and use of animals for scientific purposes. The *in situ* transcardiac perfusion was performed as previously described (24). Briefly, the mice were anesthetized with ketamine (133 mg/kg) and xylazine (10 mg/kg) intraperitoneally. The thorax was opened to expose the heart once anesthesia was established, and the descending thoracic aorta was clamped, followed by severing of both jugular veins. Perfusion fluid (pH 7.4 and warmed to 37 ºC) containing (in mM) 128 NaCl, 4.2 KCl, 1.5 $CaCl_2$, 0.9 $MgSO_4$, 24

$NaHCO_3$, 2.4 NaH_2PO_4, and 9.0 glucose was infused into the left ventricle of the heart. The perfusion rate (10 ml/min) was controlled by a Harvard infusion pump (Harvard Apparatus, Holliston, MA). After a 1 min perfusion with blank perfusion fluid (to remove plasma proteins), the mice were perfused with perfusion fluid containing [^{3}H]-diazepam (0.5 mCi/ml) for another 1 min, after which perfusions were terminated by decapitating the animal and the whole brain was harvested. Brain samples were treated overnight with 2 ml of Solvable™ at 50 ºC with hydrogen peroxide 30% (v/v) added for the final 30 min, before 10 ml of Ultima Gold scintillation cocktail was added. 200 µl of perfusate was also mixed with 2 ml of Ultima Gold scintillation cocktail. ^{3}H radioactivity was then determined using the PerkinElmer 2800TR liquid scintillation analyzer. The apparent tissue distribution volume of [^{3}H]-diazepam (B:P, ml/g) was calculated using Q_{brain}/C_p normalized by brain weight (g), where Q_{brain} is the radioactivity in the brain (DPM/g) (radioactivity from the vascular volume subtracted) and Cp is the radioactivity per ml of perfusate (DPM/ml). The vascular volume ($V_{vascular}$, ml/g) was estimated using ^{14}C-sucrose by $Q_{sucrose}/C_{sucrose}$ where $Q_{sucrose}$ is the radioactivity (DPM) of sucrose in the brain (DPM/g), and $C_{sucrose}$ is the radioactivity in perfusate (DPM/ml).

Statistical analysis of data

All data are presented as mean ± SEM. Statistical analyses were performed using GraphPad Prism 7 (GraphPad Software, San Diego, CA). Comparisons between experimental and control groups were evaluated by a Student's unpaired t test or a one-way ANOVA with a post-hoc Tukey test. Values where $p < 0.05$ were considered statistically significant and are indicated by an * in the figures.

Results

Treatment of hCMEC/D3 cells with hFABP5 siRNA did not affect cell viability

The viability of hCMEC/D3 cells following a 24 hr treatment with 5 nM of siRNA against hFABP5 was assessed using the MTT assay. As shown in **Figure 1,** no difference in the viability of hCMEC/D3 cells was observed with or without siRNA treatment. In contrast, a clear reduction in the viability of the cells was observed in the positive control group, which was hCMEC/D3 cells treated with 10% DMSO. Treating hCMEC/D3 cells with 10% DMSO led to a 95.8 ± 4.4% reduction in cell viability when compared to the control group. These results indicate that any down regulation in FABP5 or alteration to cellular uptake as a result of siRNA treatment was not associated with cell death.

hCMEC/D3 uptake of [^{3}H]-oleic, [^{14}C]-lauric and [^{14}C]-stearic acid uptake is reduced following hFABP5 siRNA treatment

qRT-PCR was performed on RNA isolated from siRNA and transfection reagent only treated hCMEC/D3 cells to assess the specificity of the siRNA against hFABP5. Using GAPDH as the housekeeping gene, the fold change of hFABP3, hFABP4 and hFABP5 mRNA between the two treatment groups were calculated from the obtained Cq values using the $2^{-\Delta\Delta CT}$. A 39.9 ± 3.8 % reduction in hFABP5 mRNA was observed **(Figure 2)**, whereas no significant effect on the mRNA of hFABP3 and hFABP4 was observed, indicating that the siRNA treatment was specific for hFABP5. While it appears that FABP3 mRNA was increased, differences were not statistically significant. A similar reduction in hFABP5 protein expression was observed from Western blots **(Figure 3)**. A noticeably lighter band at ~15 kDa, the molecular weight corresponding to FABP5, was detected in

the protein samples isolated from cells that underwent siRNA treatment. Densitometric analysis of the blots indicated that the siRNA treatment reduced the protein expression of FABP5 in hCMEC/D3 cells by 38.8 ± 6.6%.

We have previously demonstrated the genetic knockdown of hFABP5 reduces hCMEC/D3 uptake of the fatty acid DHA, albeit, using a slightly different treatment regime (24). To determine whether the current siRNA protocol had a similar impact on fatty acid uptake, the uptake of three fatty acids into hCMEC/D3 cells was investigated. This also served as a positive control for the ability of FABP5 to promote the uptake of lipophilic ligands in hCMEC/D3 cells. To ensure the impact of siRNA treatment was measured during the linear phase of fatty acid uptake, a time dependent uptake study with [^{3}H]-oleic acid on non-treated cells was performed first. The linear range of uptake of [^{3}H]-oleic acid was assumed to reflect the linear range of uptake of the other two fatty acids investigated. As shown in **Figure 4a**, the hCMEC/D3 uptake of [^{3}H]-oleic acid was linear up to 1 min, after which uptake began to plateau.

The effect of siRNA treatment on fatty acid uptake was investigated at two timepoints within this linear range (i.e. 30 sec and 1 min). Treating hCMEC/D3 cells with 5 nM hFABP5 siRNA for 24 hr significantly reduced the uptake of [^{3}H]-oleic acid, [^{14}C]-stearic acid and [^{14}C]-lauric acid **(Figure 4).** The uptake of [^{3}H]-oleic acid **(Figure 4b)** was reduced by 20.4 ± 7.4% and 41.7 ± 11.6% at 30 sec and 1 min, respectively. The uptake of [^{14}C]-stearic acid **(Figure 4c)** was reduced by 41.8 ± 11.2% and 50.7 ± 13.6% at 30 sec and 1 min, respectively. The uptake of [^{14}C]-lauric acid **(Figure 4d)** was only significantly reduced (by 37.5 ± 8.8%) at 1 min.

Reduced FABP5 expression did not impact on the hCMEC/D3 cellular uptake of diazepam, pioglitazone and troglitazone

The time dependent uptake studies indicated that hCMEC/D3 uptake followed a relatively linear function up to 1 min for [^{3}H]-diazepam, up to 30 sec for troglitazone and up to 10 min for pioglitazone after which uptake began to plateau **(Figure 5a-c).** In contrast to the reduced uptake of oleic, stearic and lauric acid observed in siRNA treated cells **(Figure 4),** no impact on hCMEC/D3 uptake of [^{3}H]-diazepam, pioglitazone and troglitazone uptake were observed **(Figure 5d-f),** despite a 39% reduction in FABP5 protein levels. To confirm that this lack of effect on drug uptake was representative of that occurring *in vivo*, the BBB transport of [^{3}H]-diazepam was measured in WT and FABP5-/- mice, the latter having previously been shown to exhibit a lower BBB transport of [^{14}C]-DHA(24). In line with the *in vitro* studies, the BBB transport of [^{3}H]-diazepam was not significantly different between WT and FABP5-/- mice **(Figure 6)**.

Discussion

Fatty acids are incorporated into phospholipids by neurons, astrocytes and pericytes, with the composition of fatty acid directly influencing membrane fluidity and membrane excitability of the cells. Fatty acids are also used as precursor molecules for lipid messengers (e.g. prostaglandins) either as second messengers of neuronal signalling pathways or direct modulators of inflammatory responses (31, 32). Dietary fatty acids represent the major source from which the central pool of brain fatty acids are derived, and therefore, effective uptake and transport mechanisms at the BBB are essential to meet the metabolic demands of the CNS (18, 32). Intracellular binding proteins such as FABPs are core components in facilitating the uptake of fatty acids across biological membranes (18), including the BBB (24, 25). We have previously described the gene and protein expression profiles of FABP3, FABP4 and FABP5 in hCMEC/D3 cells, with FABP5 appearing to exhibit the highest expression (23-25) .Furthermore we have also previously reported that FABP5 is capable of binding to a wide range of structurally diverse lipophilic drugs using an 8-Anilinonaphthalene-1-sulfonic acid (ANS) competitive displacement assay (23). In light of the functional role of FABP5 in fatty acid transport across the BBB, the purpose of the current study was to investigate whether FABP5 is involved in the cellular uptake of lipophilic drugs.

Several methods have been reported in the literature to assess the function of FABP5, including knock out mouse models (26, 33, 34), siRNA down-regulation and pharmacological treatment of primary and immortalized cells (24, 25, 35). We elected to use a siRNA approach in hCMEC/D3 cells since we have previously shown functional involvement of FABP5 in the hCMEC/D3 uptake of [^{14}C-DHA] using this approach (24).

Previously we have reported a siRNA-mediated reduction in FABP5 mRNA and protein expression in hCMEC/D3 cells of 53% and 45%, respectively, with no morphological changes following a 96 hr treatment with 5 nM siRNA (24). These results were consistent with the extent of downregulation achieved in primary BCECs reported in the literature using the same protocol (25). In the current study, we modified the existing method to investigate whether a 24 hr treatment with 5 nM siRNA could similarly reduce levels of FABP5, and therefore serve as a more rapid approach to investigate the impact of FABP5 downregulation on cellular uptake. An approximate 40% reduction in FABP5 mRNA **(Figure 2)** and protein expression **(Figure 3)** was achieved with the current (24 hr) protocol. Furthermore, no off targets effects of FABP5 siRNA on FABP3 and FABP4 were observed and no toxic effects on hCMEC/D3 cells were evident, as suggested from the MTT assay **(Figure 1)**. The new treatment regime therefore allows for greater throughput in investigating cellular function of FABP5 relative to our previous method, whilst maintaining a similar extent of knockdown.

As anticipated, a reduction in FABP5 expression led to a reduction in fatty acid uptake in siRNA treated hCMEC/D3 cells **(Figure 4)**. These results are consistent with literature evidence that demonstrates hFABP5 preferentially binds and transports long chain fatty acids (21, 36, 37). In Transwell experiments using human primary BCECs, the reduction in oleic acid transport with siRNA treatment was similar to that reported here in hCMEC/D3 cells, suggesting similarities between uptake in hCMEC/D3 cells and transport across primary human BCECs (25). In our limited data set, the reduction in uptake of fatty acids due to hFABP5 knockdown appears to correlate to the binding affinity of the fatty acids to FABP5. While only the binding data for stearic and oleic acid to hFABP5 is

available from the literature **(Table I)**, the 5.5-fold greater affinity of hFABP5 for stearic acid relative to oleic acid, is consistent with the greater impact of FABP5 down-regulation on stearic acid relative to oleic acid at 30 sec and 1 min **(Figure 4)**. The binding affinity of mFABP5 to lauric, oleic and stearic acid are available from the literature (**Table I)**, however, species-specific differences in binding to FABP5 has been reported, therefore attempts to correlate the binding of the fatty acids to mFABP5 with the extent of reduction in our brain endothelial cell uptake data following silencing of hFABP5 are not appropriate (21, 37).The reduction in fatty acid uptake with FABP5 down-regulation was also observed to correlate with the cLogP values of the fatty acids. The greatest reduction in uptake at both 30 sec and 1 min time points was observed for stearic acid (cLogP: 8.3; 42-51% reduction), followed by oleic acid (cLogP: 7.8; 20-42% reduction) and lastly, lauric acid (cLogP:5.1; no reduction at 30 sec and 38% reduction at 1 min). In general terms, the reduction in cellular uptake of these fatty acids at later timepoints with FABP5 silencing was similar to the extent of reduction in FABP5 protein expression. In summary, the impact of FABP5 in facilitating the hCMEC/D3 uptake of fatty acids appears to be correlated with the binding affinity of the fatty acids for FABP5 and the cLogP of the fatty acids.

Having demonstrated that FABP5 plays a functional role in the hCMEC/D3 uptake of fatty acids, we next sought to determine whether a similar role would be seen for lipophilic drugs. Of the drugs we had previously assessed for binding affinity to hFABP5, pioglitazone and troglitazone bound with relatively high affinity compared with other drugs, with diazepam binding with much lower affinity (23). We therefore hypothesised that FABP5 knockdown might be expected to have a greater impact on troglitazone (K_i 1.00 µM) uptake into hCMEC/D3 cells than on pioglitazone (K_i 11.0 µM), with least

impact on diazepam (K_i 325 µM). However, no reduction in the hCMEC/D3 uptake of any of the drugs was found in siRNA treated cells when assessed during the linear phase of uptake **(Figure 5d-f)**. The simplest explanation for these results would be that hFABP5 contributes little to the cytosolic uptake of its weakly binding ligands in hCMEC/D3 cells. This interpretation however does not adequality explain the discrepancy we observe between the oleic acid and troglitazone data. As detailed in **Table 1**, the binding affinity of troglitazone is similar to that of oleic acid to hFABP5. Given a 20-40% reduction in oleic acid uptake was achieved with siRNA treatment, a similar reduction in troglitazone uptake was to be expected. As seen in **Figure 5**, this was not the case. A theory which better explains the uptake results is that hFABP5 contributes little to, or is not required for the partitioning of ligands which have sufficient aqueous solubility (e.g. clogP <5) into hCMEC/D3 cells. Troglitazone has a cLogP value of 5.1 whereas oleic acid has a cLogP value of 7.8 **(Table 1).** The greater membrane to cytosol diffusivity of troglitazone over oleic acid may therefore offset the impact that FABP5 reduction has on the accumulation of troglitazone in the cytosol of hCMEC/D3 cells. This explanation would also explain why (despite having a binding affinity 10 times lower than that of troglitazone against hFABP5), pioglitazone (cLogP: 3.6) is observed to accumulate ~4.6 times more than troglitazone in hCMEC/D3 cells (after results have been corrected for initial spiking concentrations). It is also possible that the lower hCMEC/D3 accumulation of the more lipophilic troglitazone is a result of efflux activity, given that troglitazone has been reported to interact with P-gp and BCRP, which are highly expressed in hCMEC/D3 cells, yet pioglitazone does not interact with these efflux transporters (38). In summary, it appears the partitioning of hFABP5 ligands into the cytosol of hCMEC/D3 cells is not solely

dependent on the presence of FABP5. hFABP5 ligands which have sufficient aqueous solubility may be able to partition across the luminal membrane unassisted by FABP5. The interaction we have previously reported between hFABP5 and these drug is therefore limited to occur in the intercellular domain (23).

Another, albeit more speculative, explanation for the overall lack of change in drug uptake is that other iLBPs expressed in hCMEC/D3 cells which also have affinity to the drugs, i.e. FABP3 and FABP4, may mediate the cellular uptake of the drugs in compensation for the reduction in FABP5. Indeed, compensatory upregulation of FABPs in response to the specific knockout of particular FABP isoforms has been previously reported to occur in numerous cell types in FABP deficient mice models (39, 40). For example, the protein expression of FABP5 in adipose tissue is reported to be elevated in FABP4 deficient mice (39). Our PCR data from hFABP5 siRNA treated hCMEC/D3 cells however suggests that such a compensatory mechanism is not likely present at the human BBB. As seen in **Figure 2,** no elevation in the mRNA expression of hFABP3 or hFABP4 in observed in response to hFABP5 knockdown in hCMEC/D3 cells. A previous study in the literature has similarly reported no elevation to the protein expression of FABP3, FABP4 and FABP7 in brain tissue from FABP5 deficient mice (40). It is of course possible that other iLBPs or transport proteins which have not been monitored increases the transport of the drugs in response to hFABP5 knockdown. This theory is however entirely speculative and will require further investigation.

In order to positively confirm whether the results obtained *in vitro* are reflective of what would be expected *in vivo,* the BBB transport of [^{3}H]-diazepam was assessed in WT and FABP5-/- mice. Previously we demonstrated the uptake of [^{14}C]-DHA in BCEC of

mice lacking FABP5 was reduced by 48.4% relative to those obtained from WT mice (26), and the BBB transport of [^{14}C]-DHA was reduced 36.7% in FABP5-/- mice relative to WT mice using *an in situ* transcardiac perfusion technique. In the current study, we observed no differences in [^{3}H]-diazepam uptake across the BBB between WT and FABP5-/-, which is consistent with the *in vitro* uptake studies in hCEMC/D3 cells. We similarly expect no change in pioglitazone and troglitazone uptake between WT and FABP5-/- mice *in vivo*. Collectively, the results suggest there is no change in uptake for the drugs in the cells with decreased FABP5 expression and therefore their uptake process is not dependent on the presence of FABP5.

Conclusion

FABP5 is involved in the brain endothelial cell uptake of fatty acids and uptake is positively correlated with fatty acid clogP and binding affinity of the fatty acids for FABP5. Following FABP5 silencing, no change in the uptake of troglitazone, pioglitazone and diazepam into brain endothelial cells was observed, despite troglitazone having a similar binding affinity to FABP5 as oleic acid. These findings suggest that FABP5 is not essential for the uptake of these drugs in hCMEC/D3 cells and plays a limited role in the BBB trafficking of these drugs *in vivo*.

Legends to Tables

Table I. Inhibition constant K_i of the lipophilic ligands against FABP5 (mouse or human) alongside their calculated LogP values.

Legends to Figures

Figure 1. Viability of hCMEC/D3 cells transfected with 5 nM of hFABP5 siRNA complex or transfection reagent only for 24 hr. Results are represented as percentage of cells alive relative to untreated cells (control). Cells treated with 10% DMSO served as a positive control for cell death. Data are presented as mean ± SEM (n=6). *p<0.05 using a one way ANOVA with s post-hoc Tukey's test.

Figure 2. mRNA expression of FABP3, FABP4 and FABP5 in hCMEC/D3 cells 24 hr post treatment with 5 nM hFABP5 siRNA or transfection reagent only. The expression of hFABP5 mRNA was reduced by 39.9 ± 3.8%. (n=3, mean ± SEM). ***p < 0.001 using an independent samples t-test.

Figure 3. Protein expression of FABP5 in hCMEC/D3 cells 24 hr post treatment with 5 nM hFABP5 siRNA or transfection reagent only. The protein expression of FABP5 protein was reduced by 38.8 ± 6.6% (n=6, mean ± SEM). ***p< 0.001 using an independent samples t-test.

Figure 4. a) Time-dependent hCMEC/D3 cellular uptake of [^{3}H]-oleic acid, which also served as a reference profile for the time dependent uptake of [^{3}H]-lauric and [^{3}H]-stearic acid. The hCMEC/D3 cellular uptake of **b)** [^{3}H]-oleic acid, **c)** [^{14}C]-stearic acid and **d)** [^{14}C]-lauric acid were assessed during the linear phase (i.e. 30 sec and 1 min) with and without FABP5 knockdown (5 nM hFABP5 siRNA, 24 hr). Data are presented as mean ± SEM (n=4-6). * p <0.05, ** p < 0.01 using an independent samples t-test.

Figure 5. Time-dependent hCMEC/D3 cellular uptake of **a)** [^{3}H]-diazepam, **b)** pioglitazone and **c)** troglitazone. The hCMEC/D3 cellular uptake of **d)** [^{3}H]-diazepam, **e)** pioglitazone and **f)** troglitazone were assessed during the linear phase with and without FABP5 knockdown (5 nM hFABP5 siRNA, 24 hrs). Data are presented as mean ± SEM (n=4-6).

Figure 6. Brain to perfusate ratio of [^{3}H]-diazepam following *in situ* transcardiac following a 1 min perfusion with [^{3}H]-diazepam at 10 mL/min in FABP5+/+ (WT) and FABP5−/− mice. Data are presented as mean ± SEM (n=4-5).

Table I.

Compound	cLogP*	K_i
Lauric acid	5.1	mFABP5: 2.5 ± 0.53 µM[a]
Oleic acid	7.8	hFABP5: 1.6 ± 0.2 µM[b] mFABP5: 0.15 ± 0.04 µM[a]
Stearic acid	8.3	hFABP5: 0.29 ± 0.06 µM[b] mFABP5: 0.17 ± 0.04 µM[a]
Diazepam	2.9	hFABP5: 325 ± 12.0 µM[a]
Pioglitazone	3.6	hFABP5: 11.0 ± 0.06 µM[a]
Troglitazone	5.1	hFABP5: 1.00 ± 0.08 µM[a]

[a] denotes that Ki was determined by an ANS fluorescence displacement assay (23, 37)

[b] denotes that Ki was determined by a Lipidex method (36)

* cLogP was calculated using ChemBioDraw Ultra 13.0 (Cambridge Software, MA)

1 **Figure 1.**

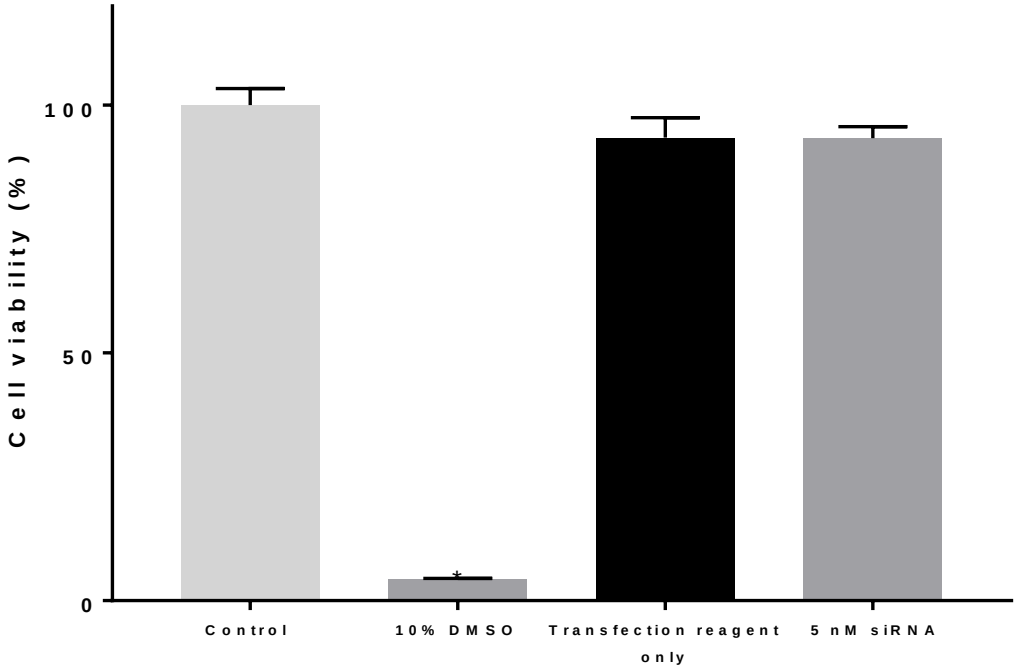
Cell viability (%)
100
50
0
*
Control
10% DMSO
Transfection reagent only
5 nM siRNA

2

Figure 2.

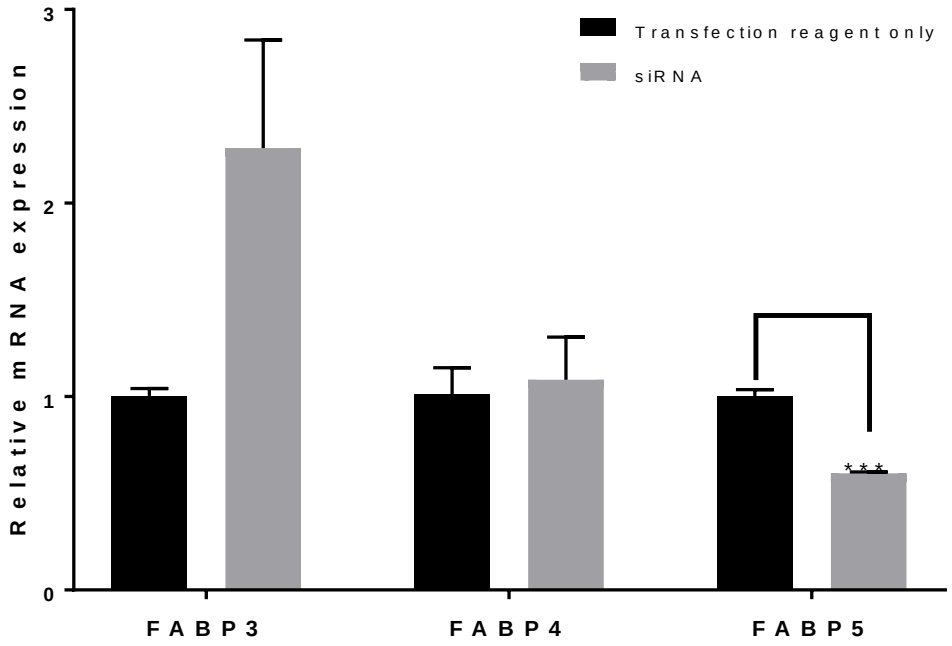
Transfection reagent only
siRNA
Relative mRNA expression
3
2
1
0
***
FABP3
FABP4
FABP5

Figure 3

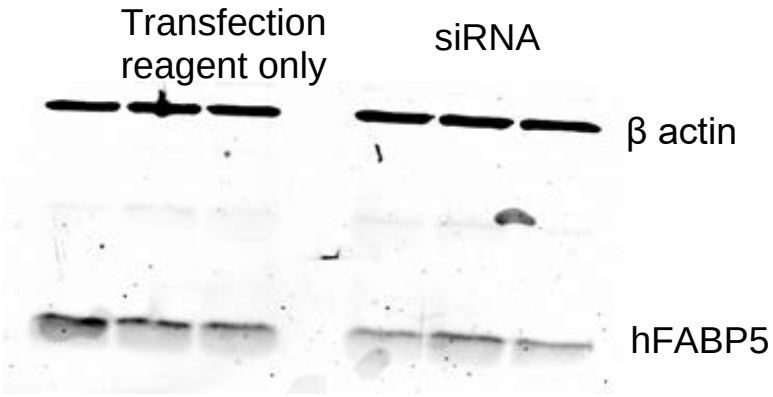
Transfection reagent only
siRNA
β actin
hFABP5

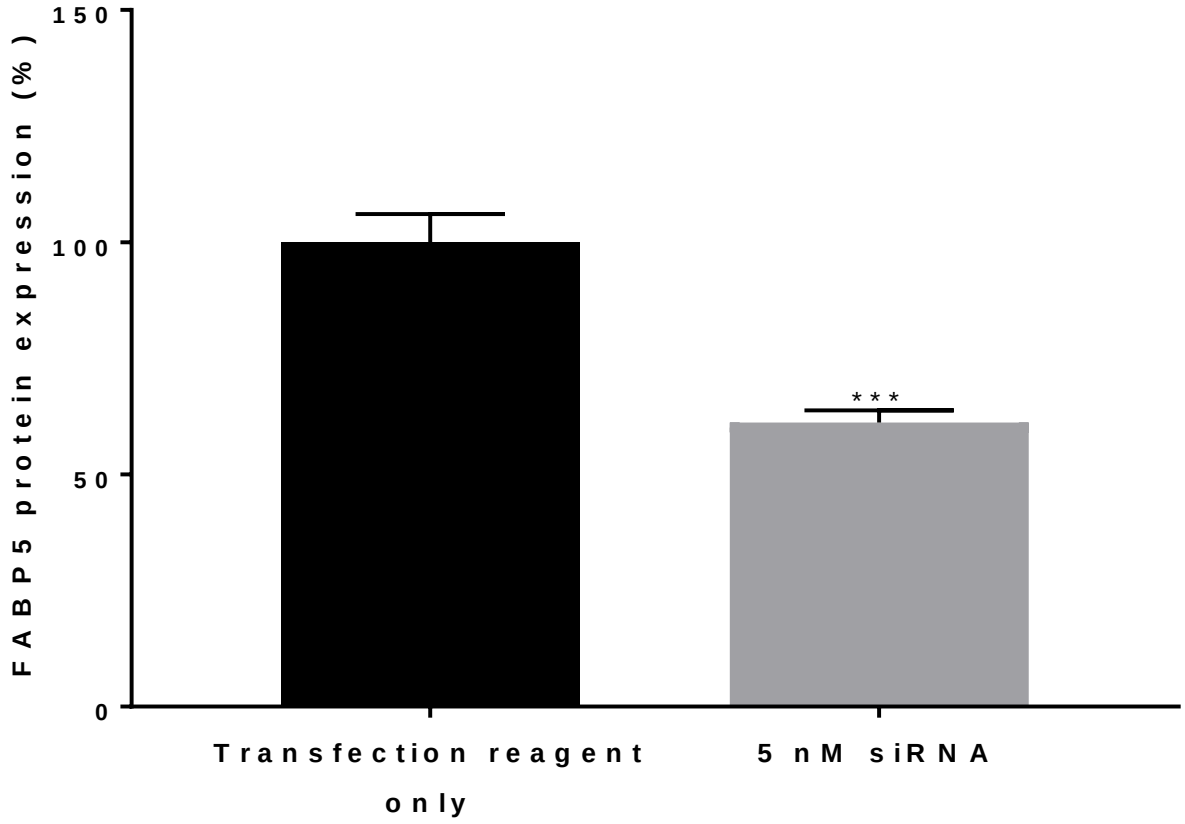
FABP5 protein expression (%)
150
100
50
0
***
Transfection reagent only
5 nM siRNA

Figure 4.

a)

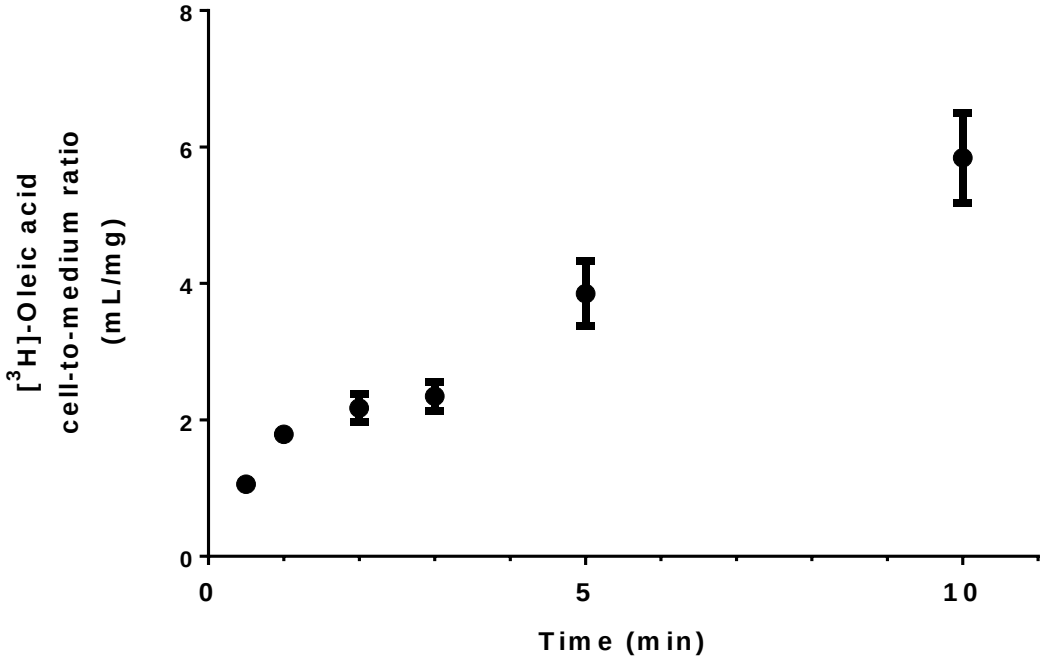

b)

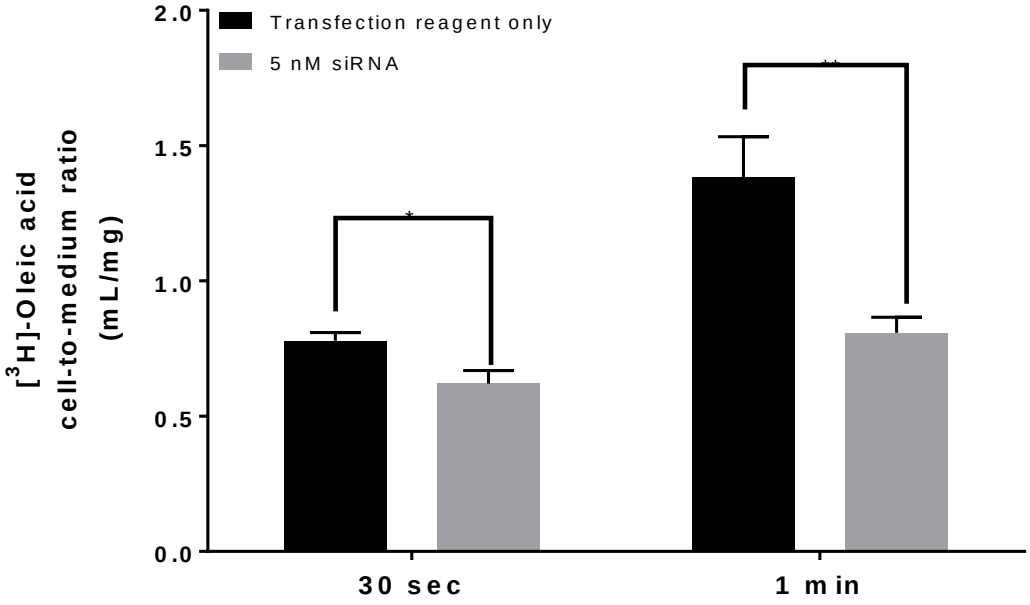
Transfection reagent only
5 nM siRNA
[3H]-Oleic acid
cell-to-medium ratio
(mL/mg)
2.0
1.5
1.0
0.5
0.0
*
**
30 sec
1 min

c)

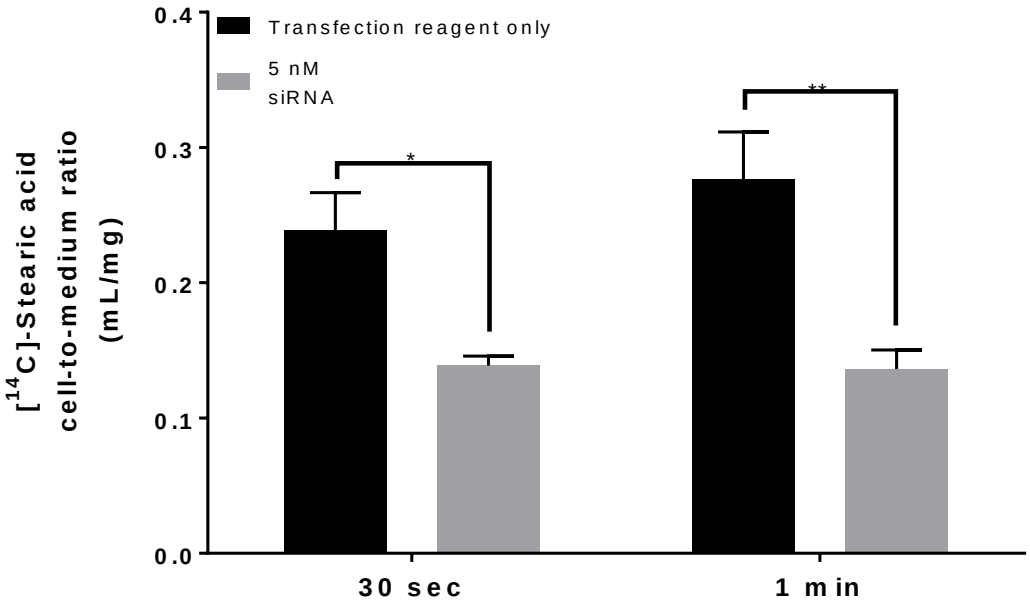
Transfection reagent only
5 nM
siRNA
[14C]-Stearic acid
cell-to-medium ratio
(mL/mg)
0.4
0.3
0.2
0.1
0.0
*
**
30 sec
1 min

d)

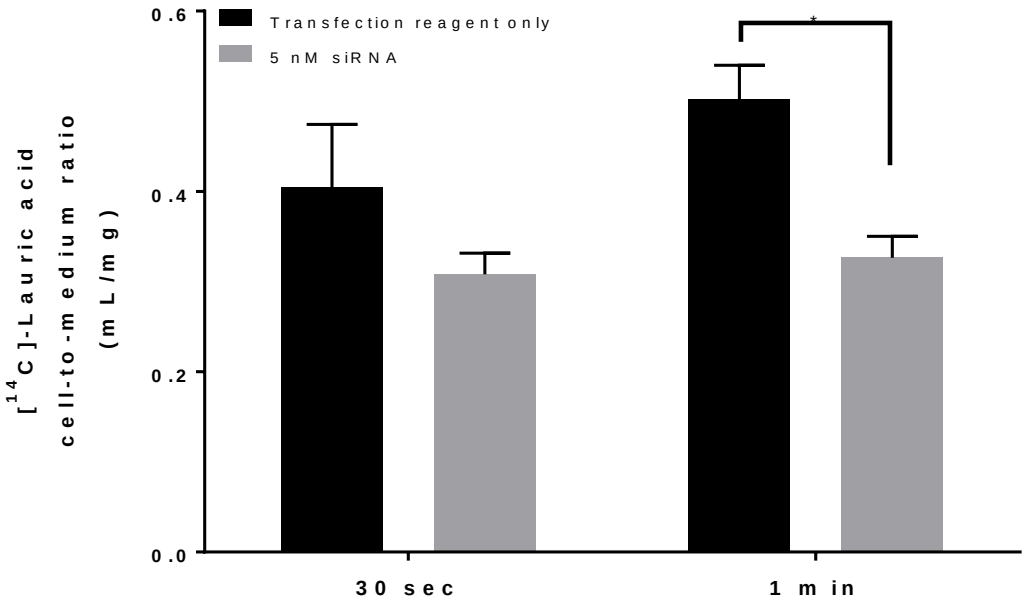
Transfection reagent only
5 nM siRNA
[14C]-Lauric acid cell-to-medium ratio (mL/mg)
0.6
0.4
0.2
0.0
*
30 sec
1 min

Figure 5.

a)

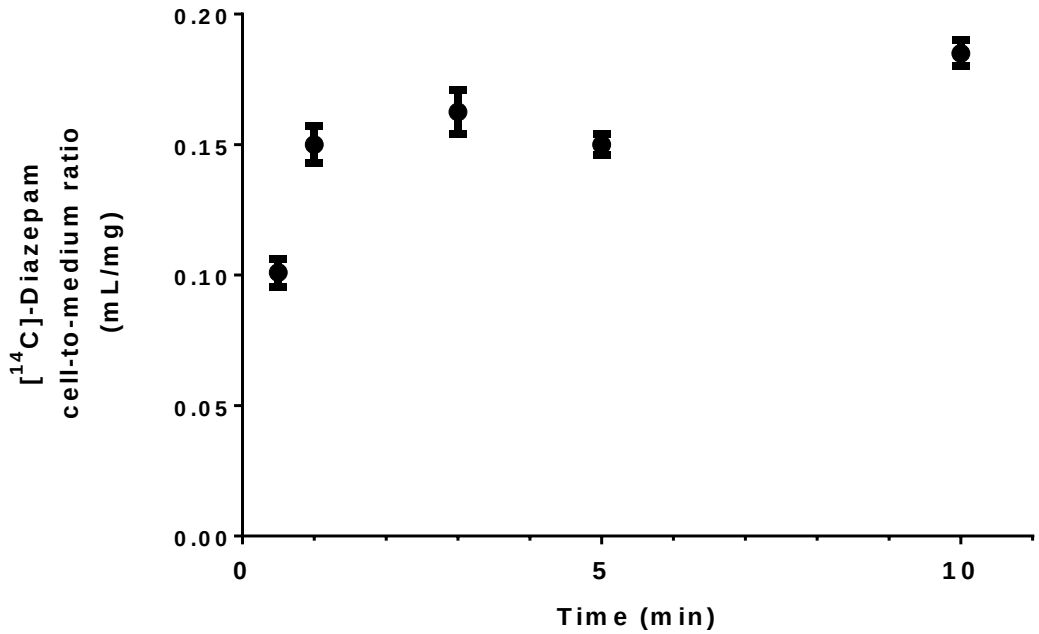
[14C]-Diazepam
cell-to-medium ratio
(mL/mg)
0.20
0.15
0.10
0.05
0.00
0
5
10
Time (min)

b)

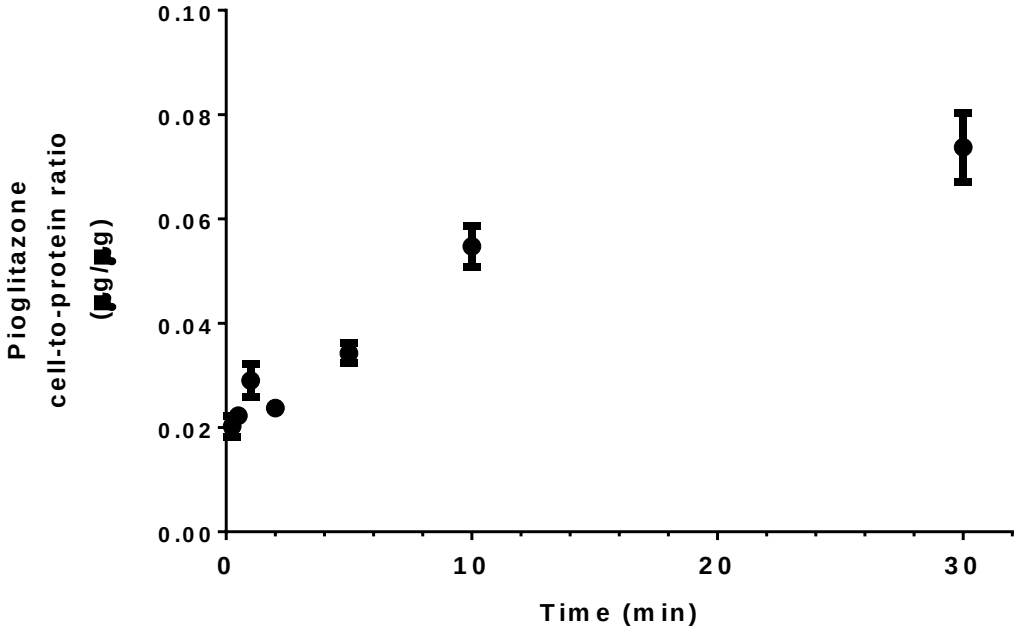
Pioglitazone
cell-to-protein ratio
(µg/µg)
0.10
0.08
0.06
0.04
0.02
0.00
0
10
20
30
Time (min)

c)

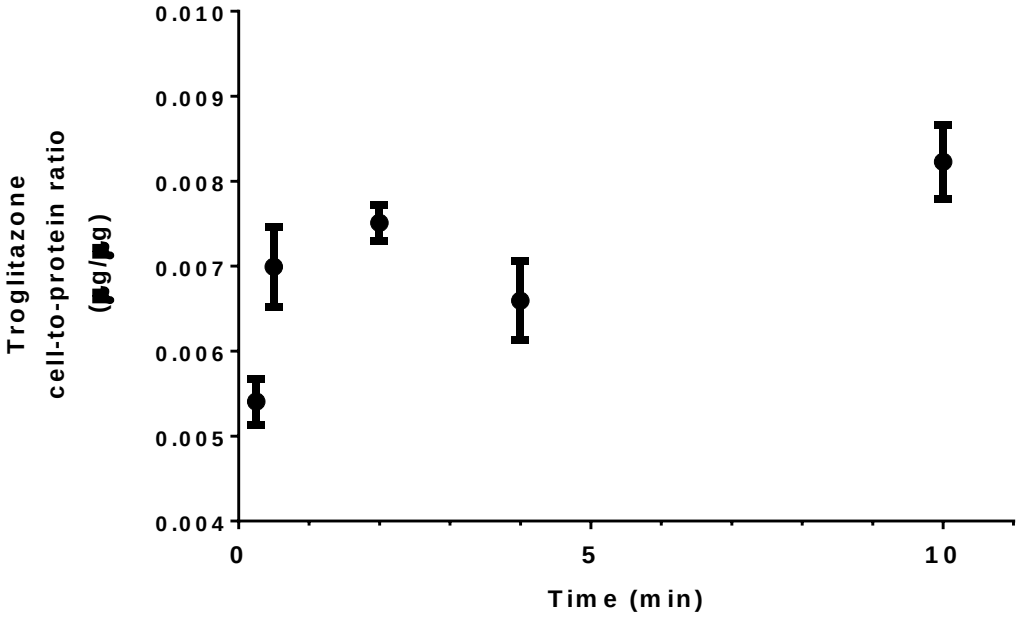
Troglitazone
cell-to-protein ratio
(µg/µg)
0.010
0.009
0.008
0.007
0.006
0.005
0.004
0
5
10
Time (min)

d)

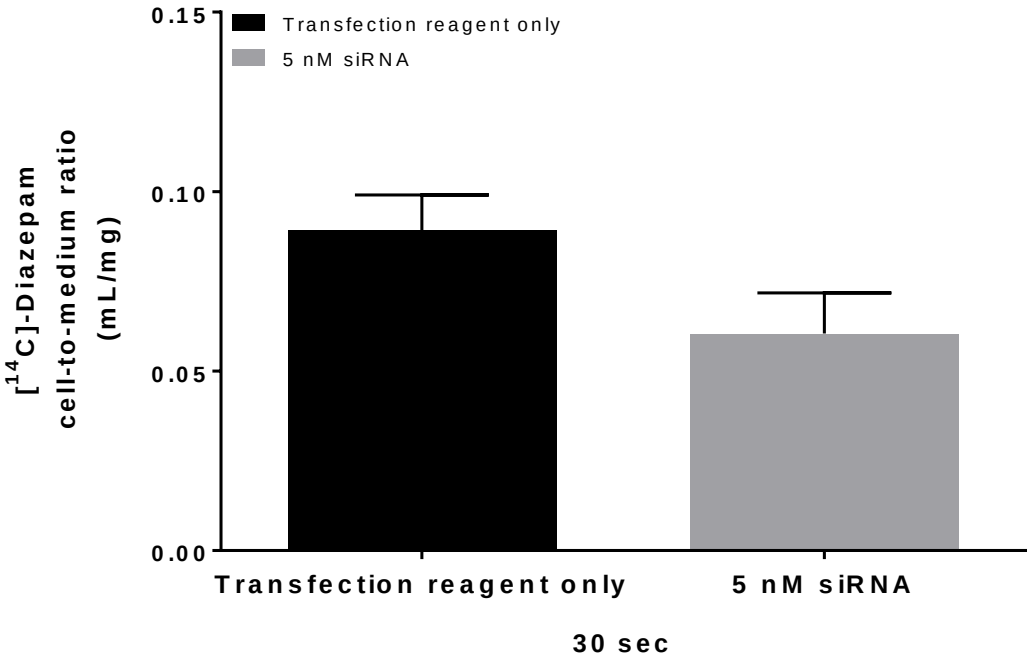
Transfection reagent only
5 nM siRNA
[14C]-Diazepam
cell-to-medium ratio
(mL/mg)
0.15
0.10
0.05
0.00
Transfection reagent only
5 nM siRNA
30 sec

e)

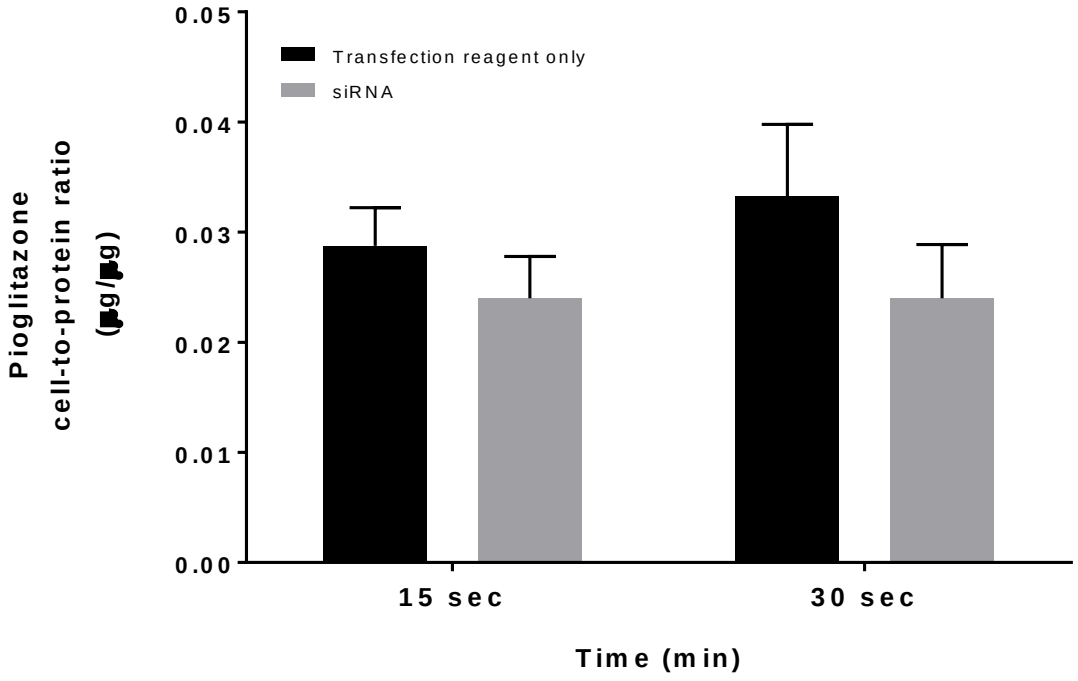
Transfection reagent only
siRNA
Pioglitazone
cell-to-protein ratio
(µg/µg)
0.05
0.04
0.03
0.02
0.01
0.00
15 sec
30 sec
Time (min)

f)

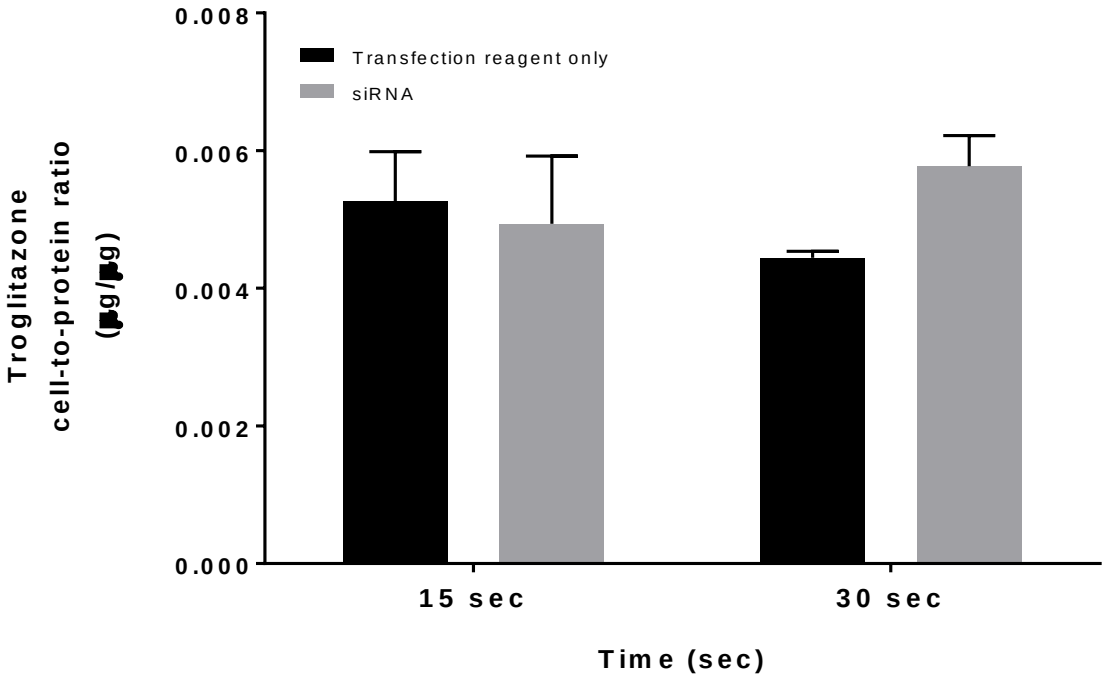
0.008
0.006
0.004
0.002
0.000
Transfection reagent only
siRNA
Troglitazone
cell-to-protein ratio
15 sec
30 sec
Time (sec)

Figure 6.

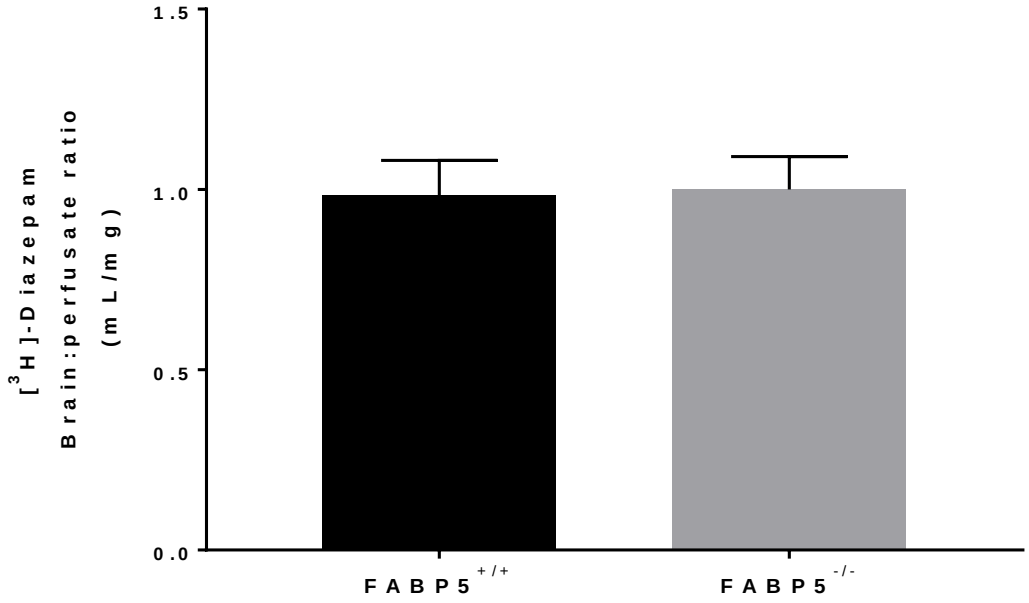
[3H]-Diazepam
Brain:perfusate ratio
(mL/mg)
1.5
1.0
0.5
0.0
FABP5+/+
FABP5-/-

References

1. Banks WA. Physiology and pathology of the blood-brain barrier: implications for microbial pathogenesis, drug delivery and neurodegenerative disorders. J Neurovirol. 1999;5(6):538-555.
2. Abbott NJ, Romero IA. Transporting therapeutics across the blood-brain barrier. Mol Med Today. 1996;2(3):106-113.
3. Pardridge WM. The blood-brain barrier: bottleneck in brain drug development. NeuroRx. 2005;2(1):3-14.
4. Abbott NJ, Patabendige AA, Dolman DE, Yusof SR, Begley DJ. Structure and function of the blood-brain barrier. Neurobiol Dis. 2010;37(1):13-25.
5. Wolburg H, Lippoldt A. Tight junctions of the blood-brain barrier: development, composition and regulation. Vascul Pharmacol. 2002;38(6):323-337.
6. Loscher W, Potschka H. Drug resistance in brain diseases and the role of drug efflux transporters. Nat Rev Neurosci. 2005;6(8):591-602.
7. Pajouhesh H, Lenz GR. Medicinal chemical properties of successful central nervous system drugs. NeuroRx. 2005;2(4):541-553.
8. Urquhart BL, Kim RB. Blood-brain barrier transporters and response to CNS-active drugs. Eur J Clin Pharmacol. 2009;65(11):1063-1070.
9. Martinez MN, Amidon GL. A mechanistic approach to understanding the factors affecting drug absorption: a review of fundamentals. J Clin Pharmacol. 2002;42(6):620-643.
10. Charles N. Diffusion and related transport mechanisms in brain tissue. Rep Prog Phys. 2001;64(7):815.

11. Hamilton JA. Transport of fatty acids across membranes by the diffusion mechanism. Prostaglandins Leukot Essent Fatty Acids. 1999;60(5-6):291-297.
12. Ochiai Y, Uchida Y, Ohtsuki S, Tachikawa M, Aizawa S, Terasaki T. The blood-brain barrier fatty acid transport protein 1 (FATP1/SLC27A1) supplies docosahexaenoic acid to the brain, and insulin facilitates transport. J Neurochem. 2017;141(3):400-412.
13. Nguyen LN, Ma D, Shui G, Wong P, Cazenave-Gassiot A, Zhang X, Wenk MR, Goh EL, Silver DL. Mfsd2a is a transporter for the essential omega-3 fatty acid docosahexaenoic acid. Nature. 2014;509(7501):503-506.
14. Velkov T, Chuang S, Wielens J, Sakellaris H, Charman WN, Porter CJ, Scanlon MJ. The interaction of lipophilic drugs with intestinal fatty acid-binding protein. J Biol Chem. 2005;280(18):17769-17776.
15. Velkov T, Horne J, Laguerre A, Jones E, Scanlon MJ, Porter CJ. Examination of the role of intestinal fatty acid-binding protein in drug absorption using a parallel artificial membrane permeability assay. Chem Biol. 2007;14(4):453-465.
16. Zimmerman AW, Rademacher M, Ruterjans H, Lucke C, Veerkamp JH. Functional and conformational characterization of new mutants of heart fatty acid-binding protein. Biochem J. 1999;344(2):495-501.
17. Zimmerman AW, Veerkamp JH. New insights into the structure and function of fatty acid-binding proteins. Cell Mol Life Sci. 2002;59(7):1096-1116.
18. Hamilton JA, Brunaldi K. A model for fatty acid transport into the brain. J Mol Neurosci. 2007;33(1):12-17.

19. Kamp F, Hamilton JA. How fatty acids of different chain length enter and leave cells by free diffusion. Prostaglandins Leukot Essent Fatty Acids. 2006;75(3):149-159.
20. Mitchell RW, Hatch GM. Fatty acid transport into the brain: of fatty acid fables and lipid tails. Prostaglandins Leukot Essent Fatty Acids. 2011;85(5):293-302.
21. Liu RZ, Mita R, Beaulieu M, Gao Z, Godbout R. Fatty acid binding proteins in brain development and disease. Int J Dev Biol. 2010;54(8-9):1229-1239.
22. Mitchell RW, Edmundson CL, Miller DW, Hatch GM. On the mechanism of oleate transport across human brain microvessel endothelial cells. J Neurochem. 2009;110(3):1049-1057.
23. Lee GS, Kappler K, Porter CJ, Scanlon MJ, Nicolazzo JA. Fatty acid binding proteins expressed at the human blood-brain barrier bind drugs in an isoform-specific manner. Pharm Res. 2015;32(10):3432-3446.
24. Pan Y, Scanlon MJ, Owada Y, Yamamoto Y, Porter CJ, Nicolazzo JA. Fatty acid-binding protein 5 facilitates the blood-brain barrier transport of docosahexaenoic acid. Mol Pharm. 2015;12(12):4375-4385.
25. Mitchell RW, On NH, Del Bigio MR, Miller DW, Hatch GM. Fatty acid transport protein expression in human brain and potential role in fatty acid transport across human brain microvessel endothelial cells. J Neurochem. 2011;117(4):735-746.
26. Pan Y, Short JL, Choy KH, Zeng AX, Marriott PJ, Owada Y, Scanlon MJ, Porter CJ, Nicolazzo JA. Fatty acid-binding protein 5 at the blood-brain barrier regulates endogenous brain docosahexaenoic acid levels and cognitive function. J Neurosci. 2016;36(46):11755-11767.

27. Trevaskis NL, Nguyen G, Scanlon MJ, Porter CJ. Fatty acid binding proteins: potential chaperones of cytosolic drug transport in the enterocyte? Pharm Res. 2011;28(9):2176-2190.

28. Velkov T. Thermodynamics of lipophilic drug binding to intestinal fatty acid binding protein and permeation across membranes. Mol Pharm. 2009;6(2):557-570.

29. Schmittgen TD, Livak KJ. Analyzing real-time PCR data by the comparative CT method. Nat Protoc. 2008;3(6):1101-1108.

30. Owada Y, Takano H, Yamanaka H, Kobayashi H, Sugitani Y, Tomioka Y, Suzuki I, Suzuki R, Terui T, Mizugaki M, Tagami H, Noda T, Kondo H. Altered water barrier function in epidermal-type fatty acid binding protein-deficient mice. J Invest Dermatol. 2002;118(3):430-435.

31. Edmond J. Essential polyunsaturated fatty acids and the barrier to the brain: the components of a model for transport. J Mol Neurosci. 2001;16(2-3):181-193

32. Haag M. Essential fatty acids and the brain. Can J Psychiatry. 2003;48(3):195-203.

33. Owada Y. Fatty acid binding protein: localization and functional significance in the brain. Tohoku J Exp Med. 2008;214(3):213-220.

34. Owada Y, Yoshimoto T, Kondo H. Spatio-temporally differential expression of genes for three members of fatty acid binding proteins in developing and mature rat brains. J Chem Neuroanat. 1996;12(2):113-122.

35. Morgan E, Kannan-Thulasiraman P, Noy N. Involvement of fatty acid binding protein 5 and PPAR β/δ in prostate cancer cell growth. PPAR Res. 2010:234629.

36. Hohoff C, Borchers T, Rustow B, Spener F, van Tilbeurgh H. Expression, purification, and crystal structure determination of recombinant human epidermal-type fatty acid binding protein. Biochem. 1999;38(38):12229-12239.

37. Liu JW, Almaguel FG, Bu L, De Leon DD, De Leon M. Expression of E-FABP in PC12 cells increases neurite extension during differentiation: involvement of n-3 and n-6 fatty acids. J Neurochem. 2008;106(5):2015-2029.

38. Weiss J, Sauer A, Herzog M, Böger RH, Haefeli WE, Benndorf RA. Interaction of thiazolidinediones (glitazones) with the ATP-binding cassette transporters P-glycoprotein and breast cancer resistance protein. Pharmacology. 2009;84(5):264-270.

39. Scheja L, Makowski L, Uysal KT, Wiesbrock SM, Shimshek DR, Meyers DS, Morgan M, Parker RA, Hotamisligil GS. Altered insulin secretion associated with reduced lipolytic efficiency in aP2-/- mice. Diabetes. 1999;48(10):1987-1994.

40. Maeda K, Uysal KT, Makowski L, Görgün CZ, Atsumi G, Parker RA, Brüning J, Hertzel AV, Bernlohr DA, Hotamisligil GS. Role of the fatty acid binding protein mal1 in obesity and insulin resistance. Diabetes. 2003;52(2):300-307.